Journal of Neurosurgery Imaging and Techniques
JNSIT, 6(1): 336-345
www.scitcentral.com

ISSN: 2473-1943

Original Research Article: Open Access

Mechanical Analysis of Peripheral Nerve: An *in vivo* Pilot Study Using Vibrational Optical Coherence Tomography

Frederick H Silver[1, 2*], Nikita Kelkar[2] and Tanmay Deshmukh[2]

[*1]*Department of Pathology and Laboratory Medicine, Robert Wood Johnson Medical School, Rutgers, the State University of New Jersey, Piscataway, NJ, USA.*

[2]*OptoVibronex, LLC., Allentown, PA, USA.*

Received June 18, 2020; Revised June 22, 2020; Accepted June 24, 2020

ABSTRACT

The objective of this study is to measure the viscoelastic properties of skin and nerve using vibrational optical coherence tomography. The mean value of the elastic modulus of several peripheral nerves was found to be 14.1 MPa +/- 1.36 MPa, which is higher than the modulus of dermal collagen (2.15 MPa), blood vessels (3.66 MPa) and fibrotic tissue (10.84 MPa).
Results of viscoelastic studies suggest that the dissipating behavior of dermal collagen, blood vessels and nerves do not explain the high dissipation of energy by skin at low strain rates (less than 50 Hz). The high dissipation of energy exhibited by skin at low strain rates is believed to be a result of reversible rearrangement of proteoglycans and water in the interfibrillar matrix that occurs when collagen fibers are stretched during loading.
It is concluded that rearrangement of the interfibrillar matrix between collagen fibers at low strain rates during skin deformation protects nervous tissue from damage as a result of mechanical overloading. It is proposed that nerve injury, healing and fibrotic tissue deposition can be followed non-invasively in vivo using VOCT.

Keywords: Skin, Virtual Biopsy, Dermal Collagen, Nerve, Biomechanics, Vibrational Optical Coherence Tomography, Vibrational OptoScope, Viscoelasticity, Energy Dissipation, Loss Modulus, Elastic Modulus, Wound Healing

Abbreviations: OCT: Optical Coherence Tomography**;** VOCT: Vibrational Optical Coherence Tomography; Stiffness: Modulus; ECM: Extracellular Matrix

INTRODUCTION

Peripheral nerves are composed of motor and sensory axons, Schwann cells and extracellular matrix (ECM) that serve a protective function during limb movement [1]. Injury to peripheral radial nerves in the arm can occur as a result humoral shaft fracture, lateral intermuscular septum compression, callus formation, fracture manipulation, compression by the lateral head of the triceps, tumors, application of a blood pressure cuff, and as a result of intramuscular injections [2]. Results of rabbit studies suggest that a compressive pressure of 50 mm Hg for 2 hours leads to minimal deterioration of the conduction velocity in the rat tibial nerve [3]. However, application of 200 to 400 mm Hg pressure for 2 hours leads to incomplete recovery of the conduction of the nerve [3]. Therefore, it is important to understand the mechanical properties of the tissue components that protect peripheral nerves from compression injuries and how these properties may affect nerve physiology and healing.

The literature on biomechanics of normal and injured nerves in humans is limited. Results of biomechanical studies on damaged mouse sciatic nerves indicate that crushed nerves initially exhibit a decrease in modulus [4]. Modulus decreases from about 7 MPa to 4.5 MPa are reported 2 days post injury; in contrast the modulus increases from 4.5 MPa to about 9 MPa as healing progresses [4]. Human optic nerve has a uniaxial tensile modulus of about 15 MPa; the inner sheath modulus is 19.8 MPa and while that of the outer sheath is 9.7

Corresponding author: Frederick H Silver, Department of Pathology and Laboratory Medicine, Robert Wood Johnson Medical School Rutgers, the State University of New Jersey 675 Hoes Lane Piscataway, NJ 08854, USA, Email: silverfr@rutgers.edu; fhsilver@hotmail.com

Citation: Silver FH, Kelkar N & Deshmukh T. (2021) Mechanical Analysis of Peripheral Nerve: An *in vivo* Pilot Study Using Vibrational Optical Coherence Tomography. J Neurosurg Imaging Techniques, 6(1): 336-345.

MPa [5]. Other surrounding skin components including cells, dermal collagen and blood vessels have lower moduli [6] than nerve, therefore it is postulated that these tissues may protect nerves from mechanical damage by dissipating impact loads through viscous processes.

Mechanical trauma to nerve can lead to acute injury; however, mechanical energy imparted to external tissues is in part dissipated by the overlying skin [7]. The skin contains a biaxial oriented collagen network containing water, proteoglycans and elastic fibers that dissipates mechanical energy through displacement of interfibrillar matrix during skin deformation [6,7]. Energy dissipation likely occurs through collagen fiber reorientation and reversible displacement of proteoglycans and water in the extracellular matrix [6,7]. Skin protects underlying tissue components from damage especially at low strain rates [Dunn and Silver, 1983]. Viscous dissipation of energy by collagen fibers found in human decellularized dermis is only about 20% of the elastic component [8]; this is much lower than the 50% observed when skin is tested in vitro using uniaxial tensile testing [7].

The purpose of this paper is to report the results of pilot studies to evaluate the biomechanics of skin and peripheral nerves in vivo using a new technique termed vibrational optical coherence tomography (VOCT). The results reported suggest that the mean elastic modulus of different peripheral nerves is 14.1 MPa ± 1.36 MPa. It is concluded that at low strain rates the viscous behavior of skin interfibrillar matrix provides a means to protect underlying tissue components including nerves from mechanical damage during impact loading.

METHODS

Subjects

Tests were conducted on the skin and peripheral nerves of 8 volunteers with ages ranging from 24 to 70 after informed consent was obtained. All studies were conducted at 75°F and 40% to 50% relative humidity. Tissues studied in vivo include skin, medial, radial, sural, and facial nerve. All reported resonant frequencies and moduli are averages from 3 to 5 different individuals.

Ultrasound Images

Subcutaneous tissues are identified from ultrasonic images obtained at a frequency of 7.5 MHz as described previously using a linear probe [6]. Ultrasound images were color coded for better visualization of the nerves by assigning different colors based on the pixel intensities.

VIBRATIONAL OPTICAL COHERENCE TOMOGRAPHY (VOCT) AND VIBRATIONAL ANALYSIS *in vivo*

Measurement of the elastic modulus

VOCT is a non-invasive and non-destructive method that uses infrared light and audible sound to create a displacement of skin as described in detail previously [6,8-10]. The displacement of the skin causes vibrations in subcutaneous tissues that are reflected back to the skin. The result is a spectrum of resonant frequencies that are recorded by measuring the displacement of the skin as a function of frequency [6]. The measured resonant frequencies are converted into modulus values using a calibration equation (equations 1 and 1a) developed based on in vitro uniaxial mechanical tensile testing and VOCT measurements on the same sample [8-19]. The modulus measured using VOCT is an elastic modulus [6].

A Vibrational OptoScope (OptoVibronex, LLC) was used to make VOCT measurements on skin over various locations above different peripheral nerves. The nerve location is identified using the ultrasound linear probe. The VOCT hand piece is then placed at the same location used to image the nerve using ultrasound. A frequency generating app is downloaded onto the i5 processor within the OptoScope. This app is capable of driving the speaker between 50 and 20,000 Hz [8-19]. The hand piece and speaker are placed over but not touching the areas of skin to be studied. During in vivo measurements, no sensation of the light or sound is felt impinging on the skin.

An OCT scanning image of the skin is obtained to ensure that the epidermis and dermis are normal [8-19]. The OptoScope system uses a fiber-coupled superluminescent diode light source with an 810 nm center wavelength and 100 nm bandwidth (full-width at half maximum) [8-19]. Although the infrared light only penetrates about 0.5 to 1 mm into the skin, the audible sound will penetrate up to about 8.0 cm through the subcutaneous tissues. For measurement of the resonant frequency and viscoelasticity of a material, the OptoScope is operated in the B mode with the beam focused on one point with a diameter of about 14 μm as previously indicated with an area should read a width [8-19].

The resonant frequency of each sample is determined by measuring the displacement of skin resulting from sinusoidal driving frequencies ranging from 50 Hz to 300 Hz, in steps of 10 Hz. The peak frequency (the resonant frequency), f_n, is defined as the frequency at which the displacement is maximized as discussed previously [8-19]. The moduli of skin and nerves are calculated from measurements of f_n using equation (1a).

The moduli are calculated from equation (1a) where E is in Pa (Pascals) and d, the thickness, is in meters. Calibration measurements were made in vitro using results of stress-strain and VOCT analyses [8-19]. The material's elastic modulus (E), determined from vibrational measurements, is related to the resonant frequency f_n through equation (1) where m, L, and A, are the mass, length, and cross-sectional area of the sample, respectively as discussed previously [8-19].

$$E = m(2\pi f_n)^2 \left(\frac{L}{A}\right) \quad (1)$$

Moduli determined using equation (1) were plotted against the corresponding moduli obtained from the tangent to the tensile stress-strain curves for all calibration materials tested as previously discussed [8-19]. These measurements were used to develop the calibration equation (1a) for tissues. Since most soft tissues have a density very close to 1.0 equation (1) becomes:

$$E * d = 0.0651 * (fn^2) + 233.16 \quad (1a)$$

The skin thickness (d) is determined from the OCT image and is used for determination of the modulus in equation (1a). Weighted displacement versus frequency data becomes a mechanical and vibrational spectrum generated by the components of the tissues that are vibrated [6]. Weighted displacement is normalized by dividing by the displacement of the speaker in the absence of the sample to correct for the displacement of the speaker as a function of frequency.

Measurement of the loss modulus

For viscous component measurements, samples were subjected to three mechanical pulses of an audible sine wave at frequencies between 50 and 200 Hz in steps of 10 Hz. The loss modulus as a fraction of the total modulus was obtained from the driving frequency peak by dividing the change in frequency at the half height of the peak (i.e. 3db down from maximum peak in power spectrum) by the driving frequency. This method is known as the half-height bandwidth method discussed by Paul Macioce (www.roush.com/wp-content/uploads/2015/09/Insight.pdf) [8,20].

RESULTS

In this study measurements were made on skin and peripheral nerves using high frequency ultrasound to locate the area of skin directly above the nerve. Vibrational optical coherence tomography was performed using the Vibrational OptoScope (OptoScope) to evaluate the elastic and viscous components of the viscoelastic behavior. A high frequency ultrasound image of the sural nerve is shown in **Figure 1**. Note the presence of the sural artery near the nerve; during ultrasonic evaluation of the nerve, the accompanying sural artery is seen to pulse in real time images. The nerve and artery are about 2.1 and 2.2 mm in diameter, respectively. The ultrasound image is color coded based on the pixel intensity to give better definition to the image of the nerve.

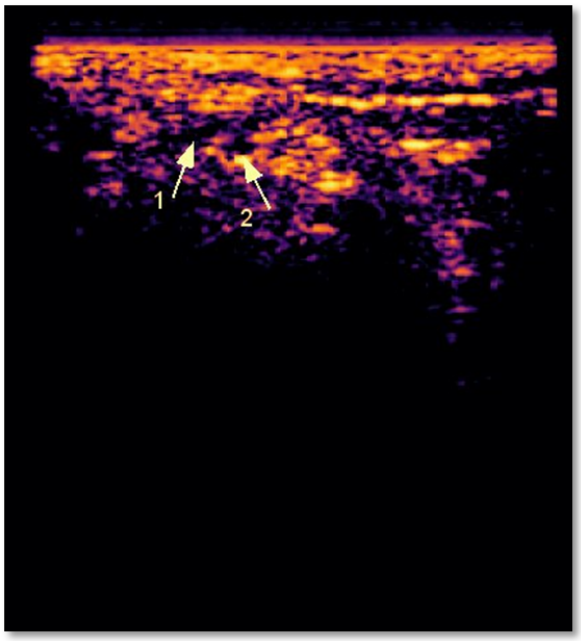

Figure 1. High frequency ultrasound image of the sural nerve. Note the location of the nerve (arrow 1) and sural artery (arrow 2). The sural artery can be observed to pulse in real time in the ultrasound image. The image was obtained using a linear probe at a frequency of 7.5 MHz.

Weighted displacement versus frequency curves for sural and medial nerves are shown in **Figure 2**. Each of the major peaks represents the behavior of a single component of the tissue that vibrates maximally at that frequency [6]. The sural nerve is characterized by two major peaks: one at about 110 Hz and the other at 280 Hz. The vascular peak at 150 Hz is present but it is small. The weighted displacement versus frequency curve for the medial nerve has four major peaks; they are found at about 110, 170, 220 and 270 Hz. The assignment of the peaks by Silver et al. [6] are 110 Hz (dermal collagen elastic modulus 2.6 MPa), 150 Hz (blood vessel elastic modulus 3.66 MPa), 220 Hz (fibrous tissue elastic modulus 10.84 MPa), and 280 Hz (nerve elastic modulus 12.45 MPa). The difference in the weighted displacement versus frequency plots for different nerves is explained by the number of tissues present in the optical window below the OptoScope hand piece. In the case of the sural nerve, the number of tissues surrounding the nerve is fewer than found in the medial nerve. The exact value for the resonant frequency of a tissue depends on the skin thickness

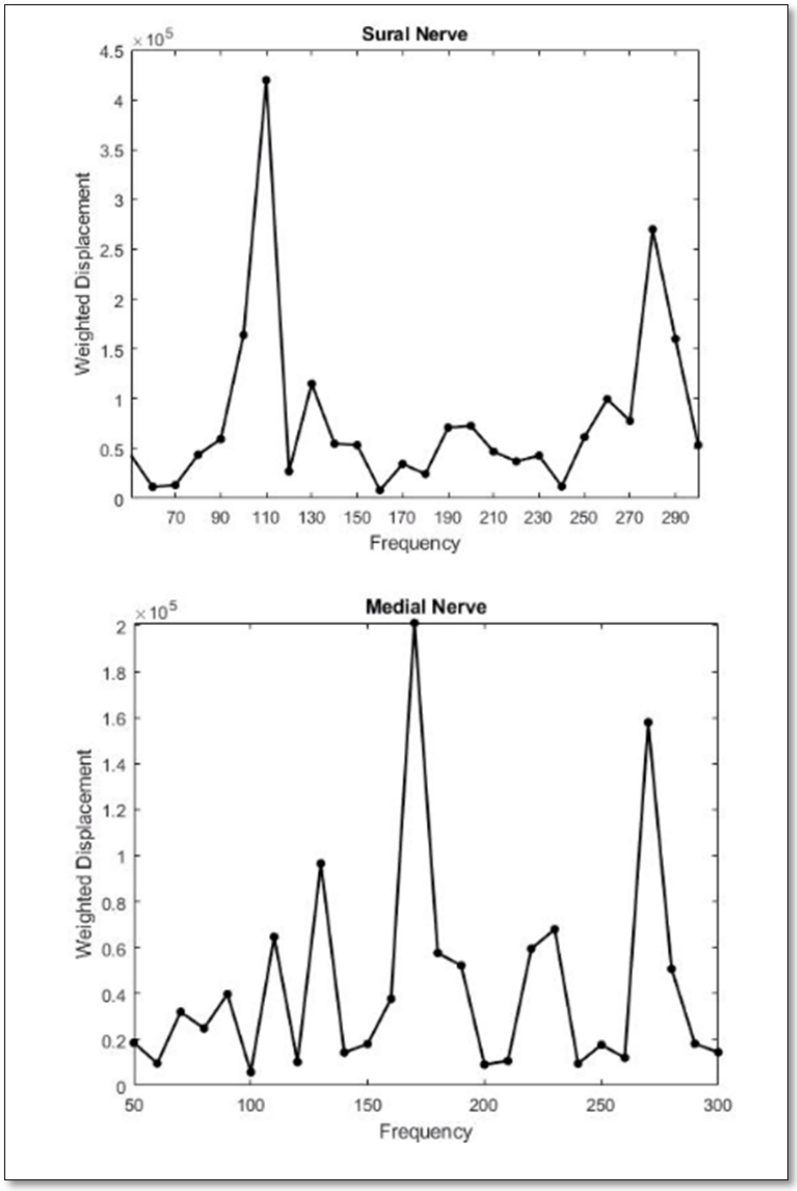

Figure 2. Weighted displacement versus frequency curves for sural and medial nerves. Each of the major peaks represents the behavior of a single component of the tissue. The major component of the sural nerve is dermal collagen (100 Hz) and nerve (280 Hz). For the medial nerve the components are dermal collagen (110 Hz), blood vessels (170 Hz), fibrous tissue (220 Hz) and nerve (270 Hz).

which varies based on the anatomical location (see equation (1a)). In contrast, the tissue elastic modulus (stiffness) of skin is about 2 to 3 MPa and does not depend on the thickness [6].

Figure 3 shows plots of the loss modulus obtained by applying an oscillating tissue mechanical loading as a function of frequency. The elastic modulus represents energy stored during tissue deformation while the loss modulus reflects energy dissipated during tissue loading. Elastic energy is stored in the tissue during mechanical loading and returned to the tissue when the load is removed [6,7]. The energy dissipated by viscous processes is converted into heat or permanent structural changes such as compressive injury or tearing. The fraction of energy lost was found at to be very small at the resonant frequency (280 Hz) for the sural and radial nerves. The low energy dissipated at 280 Hz by nervous tissues suggests that most of the energy dissipated at low strain rates is by other skin components. Protection of nerves from mechanical damage must involve other

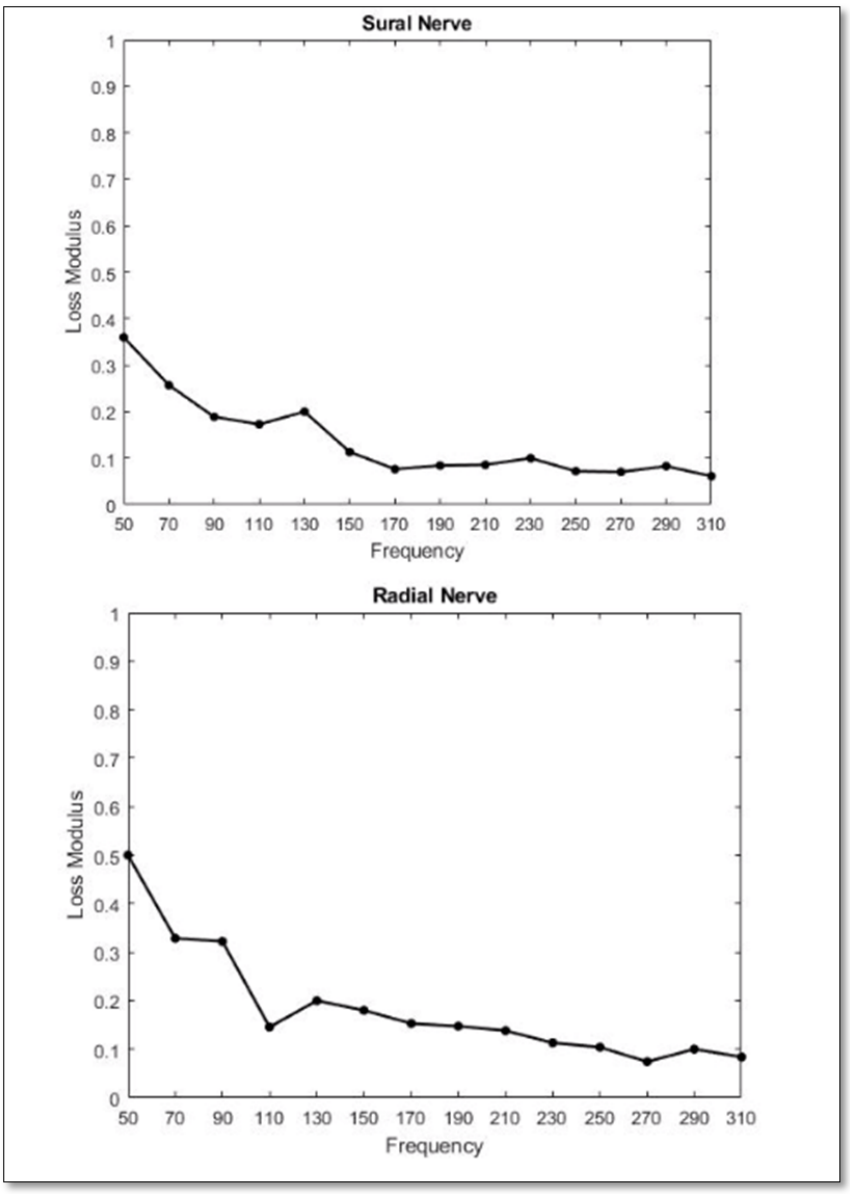

Figure 3. Plots of loss modulus versus frequency for skin over the sural and medial nerves. Note at the resonant frequency of nerve (280 Hz) the loss modulus is very small. This suggests that other components of skin besides the nerve dissipate energy during mechanical loading.

skin components at frequencies of less than 50 Hz (loading time 0.02 seconds). At the resonant frequency of nerve (280 Hz) neither the dermal collagen nor nerve can dissipate enough energy to protect the nerve from traumatic injury under mechanical loading.

Figure 4 shows a plot of weighted displacement versus frequency for skin on top of the hand **(Figure 4 top)** and skin over the radial artery **(Figure 4 bottom)**. Note on the top of the hand away from vascular tissue there is a peak at 130 Hz; the plot of weighted displacement versus frequency over the radial artery shows a peak at 100 Hz (dermal collagen) and one at about 150 Hz (vascular tissue).

Figure 5: shows plots of loss modulus as a function of frequency for skin on the top of the hand away from blood vessels **(Figure 5 top)** and skin over the radial artery **(Figure 5 bottom)**. The energy dissipated by skin decreases from 0.5 to 0.05 at frequencies between 50 Hz and 200 Hz.

Figure 6 is a plot of loss modulus versus frequency for purified decellularized dermis (dermal collagen). Note, although the loss modulus decreases from about 0.18 to

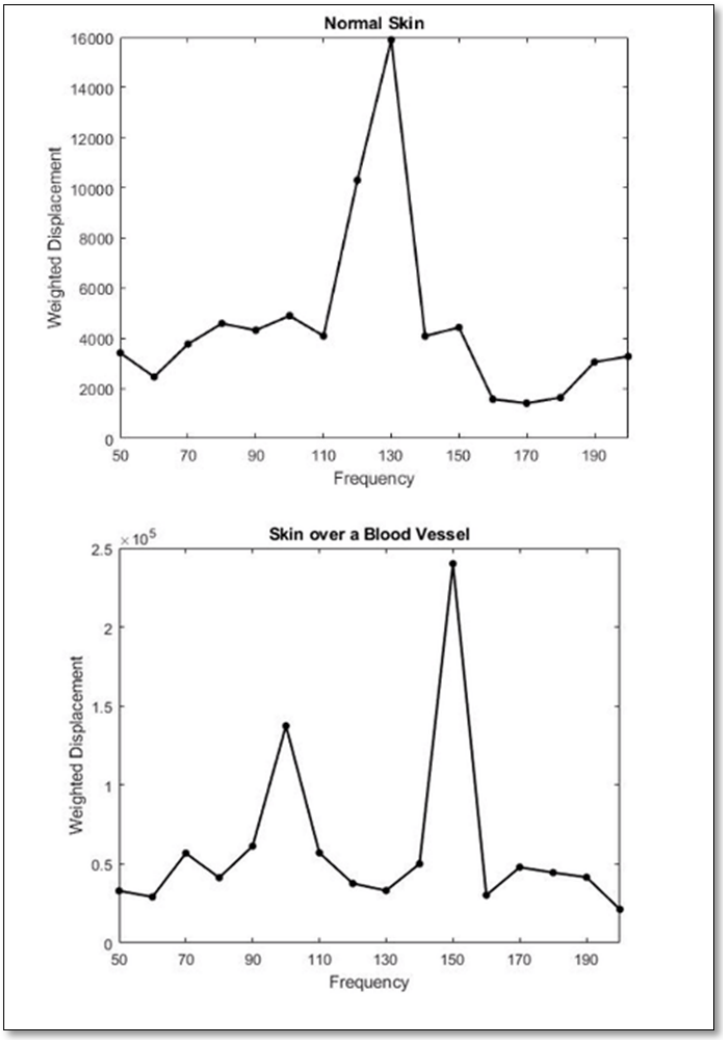

Figure 4. Plot of weighted displacement versus frequency for skin on top of the hand (Figure 4 top) and skin over the radial artery (Figure 4 bottom). Note on the top of the hand away from the radial artery the peak at 150 Hz (blood vessels) is not prominent.

about 0.08 % at the resonant frequency of collagen (100 Hz) it still is much lower than the loss modulus of intact skin which is as high as 0.5 at low frequencies **(Figure 4)**.

Figure 7 is a plot of modulus versus strain for decellularized dermis determined from VOCT measurements in vitro. The modulus of dermal collagen is between 2 to 3 MPa in skin, this is equivalent to a tissue strain of about 5% in vivo. In vivo, skin normally operates in the low strain region. In vivo scar, tissue operates in the high strain region and cannot deform and under loads.

DISCUSSION

The purpose of this study is to determine whether the modulus of different nerves can be measured non-invasively in vivo in a no touch fashion using VOCT. VOCT uses infrared light and audible sound to measure the resonant frequency of individual tissue components. The elastic modulus is then calculated from values of the component resonant frequency and the skin thickness measured from OCT images. These measurements serve as a basis for evaluating skin lesions, skin injuries and wound healing as described previously [8-19].

Our results suggest that the mechanical properties of human nerves in vivo are fairly uniform; the mean elastic modulus was found to be 14.11 MPa with a standard deviation of about 1.36 MPa. The modulus of nervous tissue is much higher than the modulus measured for cells (less than 1 MPa), dermal collagen (2 to 3 MPa), blood vessels (3 to 4 MPa), and fibrous

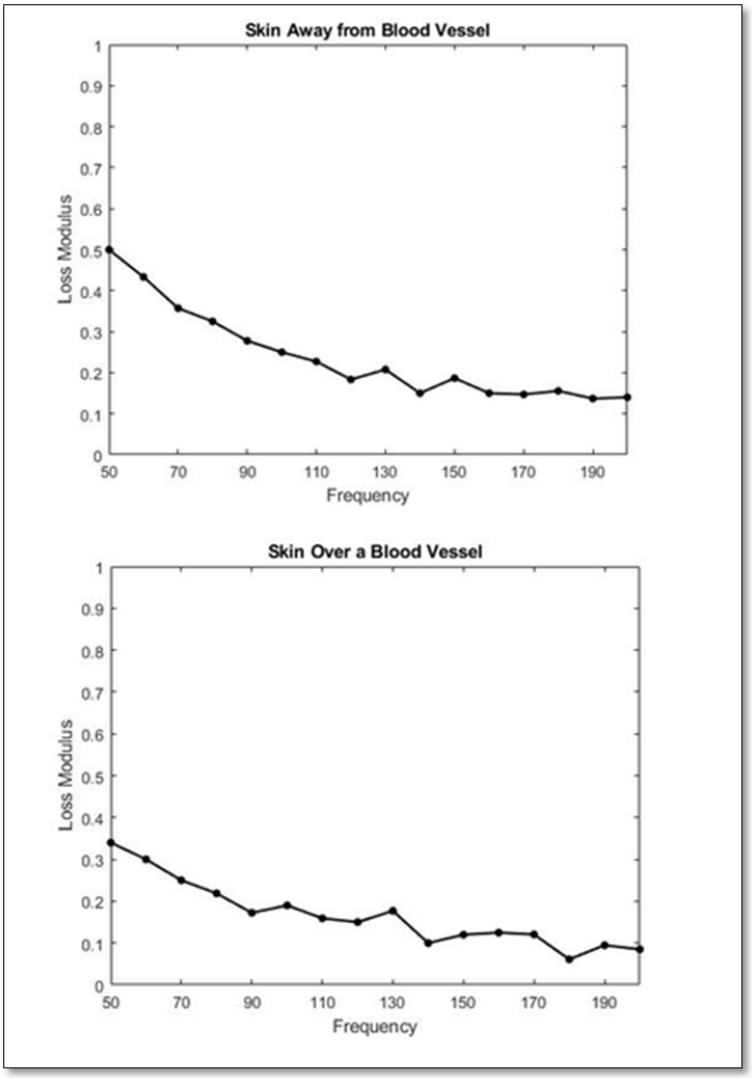

Figure 5. Plots of loss modulus as a function of frequency for skin on the top of the hand (Figure 5 top) and skin over the radial artery (Figure 5 bottom). The loss modulus based on the elastic modulus decreases from about 0.5 to 0.05 at frequencies between 50 Hz and 200 Hz.

tissue (10 MPa) [6, 8-19]. These specific values for each component provide a method to fingerprint both normal and damaged tissue elements non-invasively and non-destructively using the OptoScope.

Modulus values for soft tissues reported in vivo using other techniques such as elastography and ultrasound tend to be significantly lower than values determined from uniaxial tensile testing and therefore do not accurately measure tissue stiffness [21]. However, elastic modulus values measured in vivo using VOCT are very close to values reported for skin based on uniaxial tensile testing [6, 8-19]. In addition, using VOCT it is possible to characterize the viscoelasticity of individual tissue components found in skin and nerve in vivo. This cannot be done using elastography.

Viscoelasticity study results **(Figures 3 and 5)**, suggest that energy dissipation (loss modulus) by skin components occurs mostly at or below a frequency of 50 Hz. This indicates that protection of nerve from mechanical loading is a result of skin components other than dermal collagen, blood vessels and nerve. Decellularized human dermal collagen dissipates very little energy at any frequency **(Figure 6)**. The only other materials that could dissipate energy would be cells (50 Hz) or low molecular weight materials be such proteoglycans and water [6, 7]. Results of viscoelastic

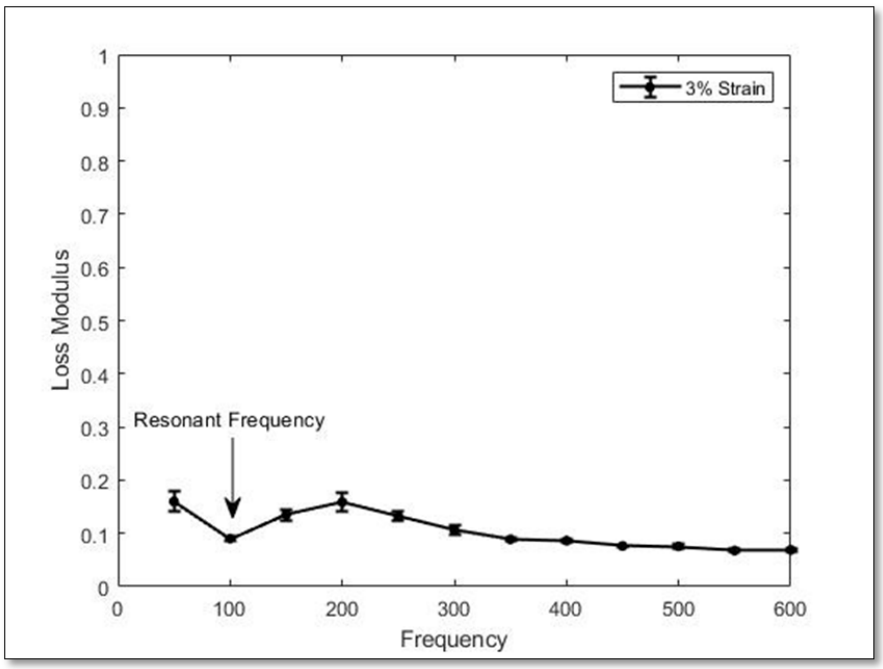

Figure 6. Plot of loss modulus versus frequency for purified decellularized dermis (dermal collagen). Note although the viscous modulus decreases from about 0.18 to about 0.08 at the resonant frequency of collagen (100 Hz) it still is much lower than the loss modulus of intact skin which is as high as 0.5 at low frequencies (Figure 4). Data modified from [8].

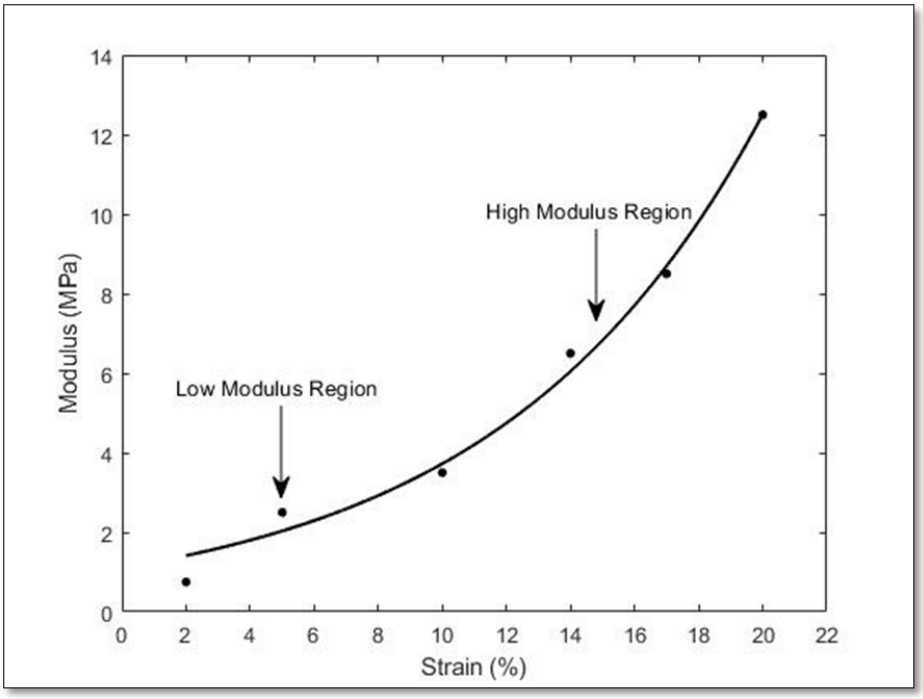

Figure 7. Plot of the modulus of decellularized human dermis versus strain determined *in vitro* from uniaxial tensile experiments. Note the *in vivo* modulus of skin determined from VOCT is between 2 to 3 MPa. Based on **Figure 7** the *in vivo* strain is about 5% and skin operates in the low modulus region of the stress-strain curve. Note the modulus of scar or fibrotic tissue is over 10 MPa and therefore scar tissue operates in the high modulus region *in vivo*. Data modified from [15].

tensile studies conducted in vitro where skin cells are not viable showed a loss modulus of about 0.5 [7]. This value is similar to the loss modulus reported in **Figure 5** with living cells. Therefore, it is concluded that it is likely that the energy dissipating ability of skin lies in rearrangement of water and proteoglycans found between the collagen fibers in the interfibrillar matrix of dermis.

In human skin, the dermal collagen forms a biaxial network that is able to rearrange reversibly without tearing during normal stretching and bending over joint surfaces [7]. During stretching, the rearrangement of water and proteoglycans as a consequence of collagen fiber reorientation, reversibly dissipates large amounts of interfibrillar material similar to that which occurs during cartilage loading. This protects skin from tearing during stretching but also protects nervous tissue from injury. Deposition of scar tissue during dermal healing limits the ability of skin to stretch [22, 23] and is expected to lead to impaired nerve repair. Therefore, by following the increase in the 220 Hz peak (scar) and loss of the peak at 280 Hz (nerve) using VOCT, one would be able to non-
invasively follow nerve regeneration and fibrotic tissue deposition.

Both natural and synthetic polymeric material-based nerve tubes are available for clinical use. The moduli and resonant frequencies of these materials are quite different than that of fibrotic and nervous tissue [6]. The healing characteristics associated with nerve entubulation devices could also be followed non-invasively using VOCT, based on the differences in the resonant frequency and moduli of the tissue components and nerve tubes.

CONCLUSION

In this pilot study we report the resonant frequencies and moduli of skin and nerve components in vivo using VOCT. The moduli of all human nerves studied are greater than that of dermal collagen, vascular, and fibrotic tissue making it possible to differentiate between these components in vivo using VOCT. Results of viscoelastic studies suggest that the energy dissipating ability of skin interfibrillar matrix protects nervous tissue from traumatic injury at low strain rates. The protective effect of skin interfibrillar materials is due to the reversible rearrangement of this matrix during skin deformation and reversible expulsion of interfibrillar fluid. It is proposed that nerve injury, healing and fibrotic tissue deposition can be followed non-invasively in vivo using VOCT.

REFERENCES

1. Topp K, Boyd BS (2012) Peripheral nerve from the microscopic function of the axon to the biomechanically loaded macrostructure. J Hand Ther 25: 142-152.
2. Latef TJ, Bilal M, Vetter M, Iwanaga J, Oskovian RJ, et al. (2018) Injury of the radial nerve in the arm: A review. Cureus 10: e2199.
3. Rydevik B, Nordberg C (1980) changes in nerve function and fibre structure induced by acute, graded compression. J Neurol Psychiatr 43: 1070-1082.
4. Beel JA, Groswald DE, Luttges MW (1984) Alterations in the mechanical properties of peripheral nerve following crush injury. J Biomech 17: 185-193.
5. Shin A, Park J, Le A, Poukens V, Demer TL (2019) Bilaminar mechanics of the human optic nerve sheath. Curr Eye Res 17: 1-10.
6. Silver FH, Kelkar N, Deshmukh T, Horvath I, Shah RG (2020) Mechano-Vibrational Spectroscopy of Tissues and Materials Using Vibrational Optical Coherence Tomography: A New Non-Invasive and Non-Destructive Technique. Recent Progress in Materials 2020; 2(2), doi:10.21926/rpm.2002010.
7. Dunn MG, Silver FH (1983) Viscoelastic behavior of human connective tissues: relative contribution of viscous and elastic components. Connect Tissue Res 12: 59-70.
8. Shah RG, Silver FH (2017) Viscoelastic behavior of tissues and implant materials: Estimation of the elastic modulus and viscous contribution using optical coherence tomography and vibrational analysis. J Biomed Tech Res 3: 105-109.
9. Silver FH, Kelkar N, Deshmukh T, Silver FH, Shah R (2020) Virtual biopsies of normal skin and thermal and chemical burn wounds. Adv Skin Wound Care 33: 1-6.
10. Silver FH, Shah RG, Richard M, Benedetto D (2019) Comparison of the virtual biopsies of a nodular basal cell carcinoma and an actinic keratosis: Morphological, cellular and collagen analyses. Adv Tissue Eng Regen Med 5: 61-66.
11. Silver FH, Shah RG, Richard M, Benedetto D (2019) Use of vibrational optical coherence tomography to image and characterize a squamous cell carcinoma. J Derm Res Ther 5: 067.

12. Shah R, Pierce MC, Silver FH (2016) A method for non-destructive mechanical testing of tissues and implants. J Biomed Mater Res A 105: 15-22.

13. Silver FH, Shah R (2020) "Virtual biopsies" of normal skin and thermal and chemical burn wounds. Adv Skin Wound Care 33: 1-6.

14. Silver FH, Silver LL (2017) Non-invasive viscoelastic behavior of human skin and decellularized dermis using vibrational OCT. Derm Clin Res 3: 174-179.

15. Silver FH, DeVore D, Shah R (2017) Biochemical, biophysical and mechanical characterization of decellularized dermal implants. Mater Sci Appl 8: 873-888.

16. Silver FH, Silver LL (2018) Use of vibrational optical coherence tomography in dermatology. Arch Dermatol Skin Care 1: 3-8.

17. Silver FH, Shah RG, Benedetto D, Dulur A, Kirn T (2019) Virtual biopsy and physical characterization of tissues, biofilms, implants and viscoelastic liquids using vibrational optical coherence tomography. World J Mech 9: 90332-90348.

18. Silver FH, Shah RG, Richard M, Benedetto D (2019) Comparative "virtual biopsies" of normal skin and skin lesions using vibrational optical coherence tomography. Skin Res Tech 25: 743-749.

19. Silver FH, Shah RG, Richard M, Benedetto D (2019) Use of vibrational optical coherence tomography to image and characterize a squamous cell carcinoma. J Derm Res Ther 5: 067.

20. Papagiannopoulos GA, Hatzigeorgiou GD (2011) On the use of the half-power bandwidth method to estimate damping in building structures. Soil Dyn Earthq Eng 31: 1075-1079.

21. Silver FH, Shah R (2016) Measurement of mechanical properties of natural and engineered implants. Adv Tissue Eng Regen Med 1: 1-9.

22. Doillon CJ, Dunn MG, Bender E, Silver FH (1985) Collagen fiber formation in vivo: Development of wound strength and toughness. Collag Relat Res 5: 481-492.

23. Dunn MG, Silver FH, Swann DA (1985) Mechanical analysis of hypertrophic scar tissue: Structural basis of apparent increased rigidity. J Invest Dermatol 84: 9-13.